
Bio-Based Soft Elastomeric Capacitor for Structural Health Monitoring Applications

Sari Kharroub

Department of Civil, Construction, and Environmental Engineering, Iowa State University, USA

Simon Laflamme

Department of Civil, Construction, and Environmental Engineering, Iowa State University, USA
Department of Electrical and Computer Engineering, Iowa State University, USA

Samy Madbouly

Department of Material Science and Engineering, Iowa State University, USA
Faculty of Science, Department of Chemistry, Cairo University, Orman-Giza 12613, Egypt

Filippo Ubertini

Department of Civil and Environmental Engineering, University of Perugia, Via G. Duranti 93, Perugia 06125, Italy

Abstract

Recent advances in flexible electronics have enabled the development of large-area electronics, which are typically fabricated from petroleum-based polymers. With the rapidly growing market of flexible electronics and sensors, there is a pressure to move towards environmentally-friendly products. In this paper, we present a bio-based polyurethane soft elastomeric capacitor (SEC) for structural health monitoring applications. The sensor's dielectric is fabricated using castor oil-based waterborne polyurethane, mixed with titanium dioxide, which replaces a petroleum-based dielectric materials (e.g. styrene-ethylene/butylene-styrene, SEBS) previously used by the authors. A critical advantage of the proposed castor oil-based polyurethane over SEBS is the environmentally-friendly nature of the bio-based polymer and water-based fabrication process of the dielectric that limits the use of solvents. Static characterization demonstrates the linearity of the sensor and its ability to transduce local strain of large surfaces into change in capacitance. Material tests results show good physical and chemical properties despite a decay of the dielectric that occurs after the first 16 days of fabrication.

Keywords structural health monitoring; strain monitoring; capacitive sensor; soft elastomeric capacitor; bio-based sensor; stretchable sensor; dielectric polymer; large area electronics

This article is from Structural Health Monitoring, 14(2), 2015: 137-147 doi:10.1177/1475921714560072. posted with permission

Corresponding author:

Sari Kharroub, Iowa State University, Town Engineering #176, Ames IA, 50011
Email address: sarikh@iastate.edu

Introduction

Structural Health Monitoring (SHM) is the automated process of structural condition assessment, aimed at replacing ineffective and judgment-dependent visual inspections. It is also considered as an improvement with respect to non-destructive evaluation techniques (Blitz, 1996) (Grosse, 2008), which are expensive and require highly-trained inspectors (Rens, 1997). Popular real-time SHM techniques include fiber-optics (Li, 2004)(Lopez, 2011)(Glisic, 2012) and piezoelectric (giurgiutiu,2007) sensors, which have shown capability of damage diagnosis, but typically require embedment. Surface sensing strategies such as accelerometers (Da, 2009) are less expensive to install, but result in a more complex signal processing task that makes damage localization difficult. An alternative is the installation of large-area electronics (LAEs), which have the potential to detect local damages over a large surface by mimicking the biological function of skin (Laflamme, 2012)(Hurlebaus, 2004)(Carlson, 2006)(Tata, 2009)(Lipomi, 2011)(Hu, 2014)(Zhou, 2011).

LAEs are enabled by recent advances in conductive polymers (Gangopadhyay, 2000). Popular applications in SHM include the utilization of carbon nanotube (CNT) nanocomposites to create resistive strain sensors (Loh, 2009)(Gao, 2010). CNT is typically used due to its strength and super-elastic attribute (Kang, 2006), but its utilization results in high fabrication costs and difficult scalability. Capacitance-based strain sensors have been proposed for various applications including strain (Arshak, 2000)(Suster, 2006), pressure (Lipomi2011), tri-axial force (Dobrzynska2013), and humidity (Harrey2002)(Hong, 2012) sensing. The vast majority of the applications utilize petroleum-based polymers (Madbouly, 2013) (Xia, 2010). However, with the rapidly growing markets of flexible electronics and sensors, there is an economic and social pressure to utilize environmentally-friendly materials to support large-scale deployments.

With the exception of castor oil, nearly all vegetable oils do not naturally have the hydroxyl groups necessary to produce polyurethane dispersions (PUDs). The carbon-carbon double bonds and the ester functionality present in triglycerides allow for the introduction of such groups, a technique leveraged in the production of the majority of the vegetable oil-based polyols. In this paper, we present a bio-based LAE for SHM applications. The sensor is a soft elastomeric capacitor, and its dielectric is constituted from a castor oil-based polyurethane (PU) mixed with titanium dioxide (TiO_2 or titania) particles. Vegetable oil-based waterborne polyurethane has recently emerged as a new branch of PU chemistry in an effort to reduce negative impacts on the environment and minimize fabrication costs. This branch has been rapidly growing, driven by the versatility and environmental friendliness of these PUs. Here, waterborne castor oil-based PUD is used in order to partly eliminate organic solvents in the SEC's fabrication process (Madbouly, 2013) (Lu, 2008) (Lu, 2005). This results in the reduction of toxic volatile organic compounds that exist in conventional PUs in significant amounts, and minimization of hazardous air pollutants (Lu, 2008). Unlike solvent-based PUDs, the aqueous PUDs can be applied with high solids content, because their viscosity does not depend on the molecular weight of polyurethane.

The proposed bio-based SEC has been developed as a possible replacement to a petroleum-based SEC previously developed by the authors, fabricated from a styrene-ethylene/butylene-styrene (SEBS) matrix. It was shown that such sensor combines the advantages of large area applications, flexibility, and robustness, which result in high scalability (Laflamme, 2012), (Laflamme, 2013). The bio-based feature of the proposed castor oil-based sensor would improve the sustainability of the SEC's materials and fabrication process. It is important to make the distinction that with this first generation only the polymer at the dielectric

level is a bio-based product. The compliant electrodes are constituted from an SEBS-carbon black mix. The dispersion of carbon black within a castor-oil substrate requires further investigation.

The paper is organized as follows. In the next section, the background of the sensor is described, which includes a description of the materials used, sensor fabrication process, and sensing principle. It is followed by a study of the sensor on a materials perspective, with a discussion on the dispersion of the filler and decay of the dielectric. Afterwards, we experimentally verify the sensor's linearity and validate its theoretical gauge factor. The last section concludes the paper.

Background

Materials

Castor oil, isophorone diisocyanate (IPDI), dimethylol propionic acid (DMPA), and dibutyltin dilaurate (DBTDL) were obtained from Aldrich Chemical Company (Milwaukee, WI). Methyl ethyl ketone (MEK) and triethylamine (TEA) were purchased from Fisher Scientific Company (Fair Lawn, NJ). SEBS was acquired from VTC Elastoteknik AB, Sweden, carbon black Printex XE 2-B from Orion Engineered Carbons (Kingwood, TX), and TiO₂ was purchased from Sachteleben Chemie GmbH (Germany). All materials were used as received without further purification or analysis.

Details about the synthesis of castor oil-based PUD can be found in our recent publication (Madbouly, 2013). Briefly, the castor oil-based PUD are synthesized by a reaction of IPDI, castor oil, and DMPA as internal surfactant. The DMPA incorporates carboxylic functionality in the

prepolymer backbone. Tertiary amine (e.g., triethylamine, TEA) is then used to neutralize the carboxylic groups and produce ionic centres to stabilize the polymer particles in water.

Castor oil-based PU is then mixed with TiO_2 , which both serve as a dielectric of the capacitor. TiO_2 , an environmentally-friendly and readily available filler (Yang,2013), is added and dispersed in the castor oil in order to increase the permittivity of the PU (Saleem, 2013). The preparation of SEC is finalized by sandwiching the dielectric with two conductive electrodes fabricated from a carbon black and SEBS mix. Figure 1 illustrates the composition of a bio-based SEC.

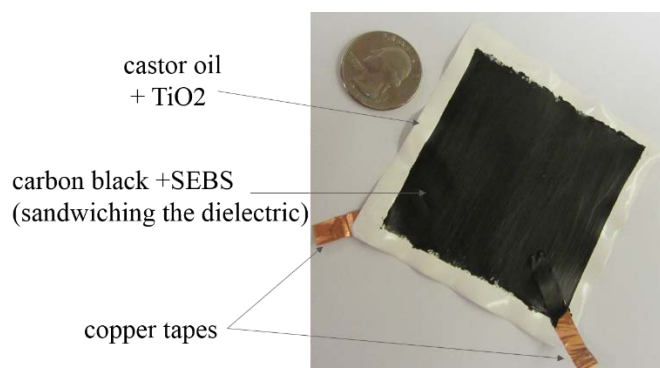


Figure 1. A single bio-based SEC

Sensor Fabrication

The sensor's fabrication process is shown in Figure 2. Firstly, the dielectric of the capacitor (castor oil doped with TiO_2) is prepared using a solution casting method. TiO_2 nanoparticles are dissolved using methanol solvent before they are added to the castor oil PU at various volume percentages (5%, 10% and 15%) and dispersed using via sonication using an ultrasonic tip. The resulting homogenous solution is drop-casted onto a glass plate and dried at room temperature for about 3 days to allow evaporation of water. Secondly, a 15 ml of

SEBS/toluene solution is added to 0.79 g of carbon black to create the compliant electrodes. A sonication bath (Branson CPXH 2800) is used to disperse the carbon black particles. Finally, the carbon black-SEBS solution is sprayed on both surfaces of the dried polymer. Two conductive copper tapes are attached to the electrodes during the drying process to create mechanical connections for connecting to the data acquisition system (DAQ).

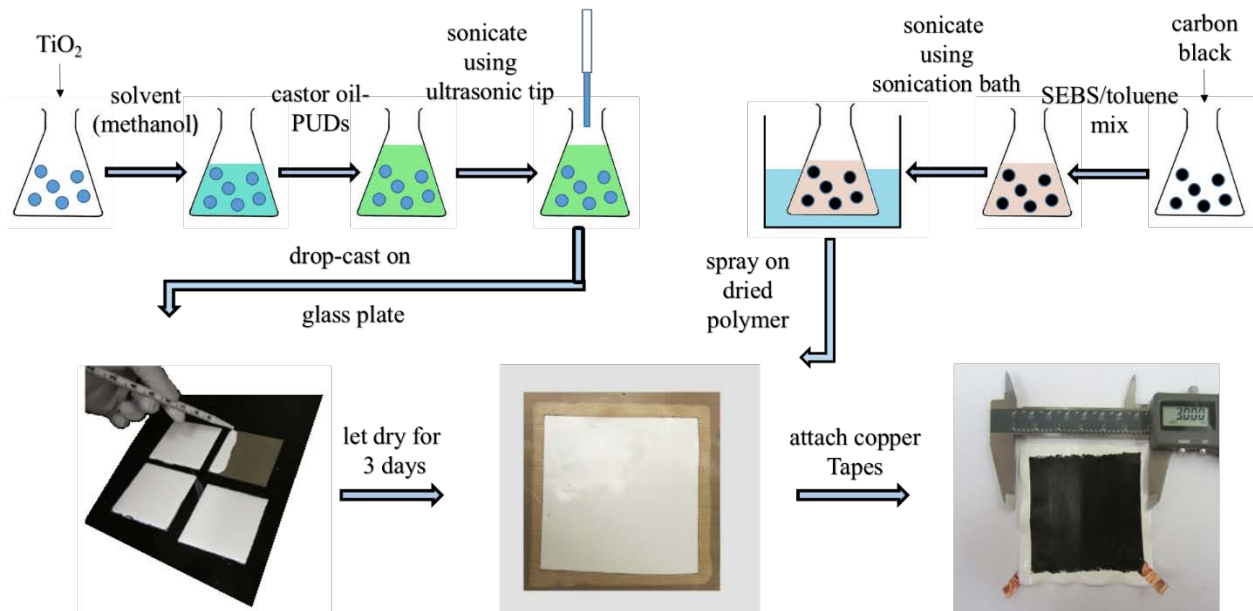


Figure 2. Sensor Fabrication

Sensing Principle

The sensor behaves as a non-lossy capacitor when operating at relatively low frequencies ($\leq 1\text{kHz}$):

$$C = \frac{e_0 e_r A}{h} \quad (1)$$

where $A = w \cdot l$ is the surface area of electrodes with width w and length l , and h is the thickness of the dielectric, $\epsilon_0 = 8.854 \text{ pF/m}$ is the vacuum permittivity and ϵ_r is the dimensionless relative permittivity of the composite. Assuming small deformation, we can take the derivative of equation (1) to obtain the following expression:

$$\Delta C = \left(\frac{\Delta l}{l} + \frac{\Delta w}{w} - \frac{\Delta h}{h} \right) C \quad (2)$$

$$\frac{\Delta C}{C} = \epsilon_X + \epsilon_Y - \epsilon_Z \quad (3)$$

where ϵ is the strain in the principal axes illustrated in Figure 3. The SEC is designed to be adhered onto the surface of the monitored structure in the x-y plane using an epoxy. Taking Hooke's Law specialized for plane stress, we obtain an expression for ϵ_Z :

$$\epsilon_Z = -\frac{\nu}{1-\nu}(\epsilon_X + \epsilon_Y) \quad (4)$$

where ν is the Poisson's ratio of the sensor. Substituting equation (4) into equation (3) gives:

$$\frac{\Delta C}{C} = \lambda(\epsilon_X + \epsilon_Y) = \frac{1}{1-\nu}(\epsilon_X + \epsilon_Y) \quad (5)$$

where λ represents the gauge factor. Equation (5) can be rearranged using equation (1) to obtain the sensor's sensitivity:

$$\Delta C = \frac{\lambda(\epsilon_x + \epsilon_y)e_0e_rA}{h} \quad (6)$$

Equation (6) shows that the sensor's sensitivity in term of measured strain can be increased by increasing the width and length of the sensor, decreasing the thickness of dielectric or increasing the permittivity. In addition, equation (5) can be specialized for uniaxial strain along the x -axis of a monitored material of significantly higher stiffness (e.g., monitoring of a concrete beam). In this case, strain in the y -axis is written as $\epsilon_y = -\nu_m\epsilon_x$, where ν_m is the Poisson's ratio of the monitored material. In this case, equation (5) becomes:

$$\frac{\Delta C}{C} = \lambda\epsilon_x = \frac{1 - \nu_m}{1 - \nu} \epsilon_x \quad (7)$$

Figure 3 illustrates the sensing of the SEC.

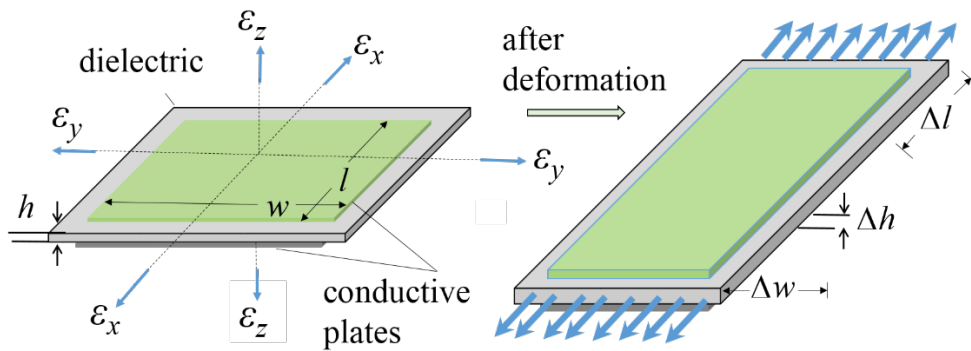


Figure 3. Sensing principle

Materials Properties

Dispersion of filler

Morphological inspection of the castor oil-based PU/TiO₂ nanocomposites was performed using scanning electron microscopy (SEM) for different TiO₂ contents. The samples were fractured in liquid nitrogen, fixed on the SEM holders, and sputtered with gold. The prepared samples were investigated using a field-emission scanning electron microscope (FE-SEM, FEI Quanta 250) operating at 10 kV under high vacuum. Figure 4 shows typical SEM micrographs for PU/TiO₂ nanocomposites with 5, 10, and 15 volume% TiO₂ to polymer contents, taken 3 days after fabrication. TiO₂ is dispersed along the horizontal axis, but appears to have settled in the vertical axis. Given the utilization of the sensor in an in-plane mode, uniform dispersion is only required along the horizontal axis, yet preferable among the entire volume. The section on laboratory verification will confirm the homogeneous in-plane dispersion of the particles by demonstrating the linearity of the sensor and verifying the theoretical gauge factor experimentally. However, the non-uniform settlement along the sensor's thickness needs further investigation. Figure 5 shows a blow up on the region where TiO₂ has settled. The micrograph shows well dispersed TiO₂ in the PU matrix with an average particle size as small as 200 nm in this region.

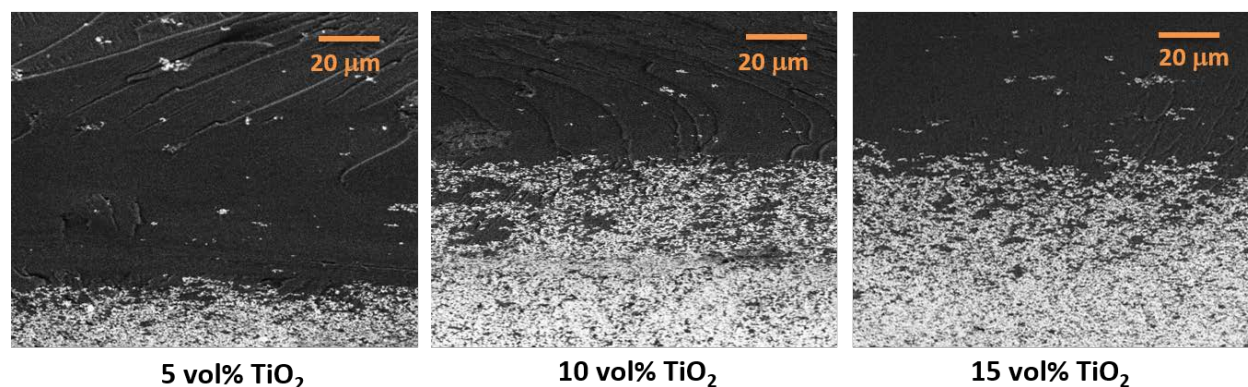


Figure 4. SEM micrographs for PU/TiO₂ nanocomposites for different composition

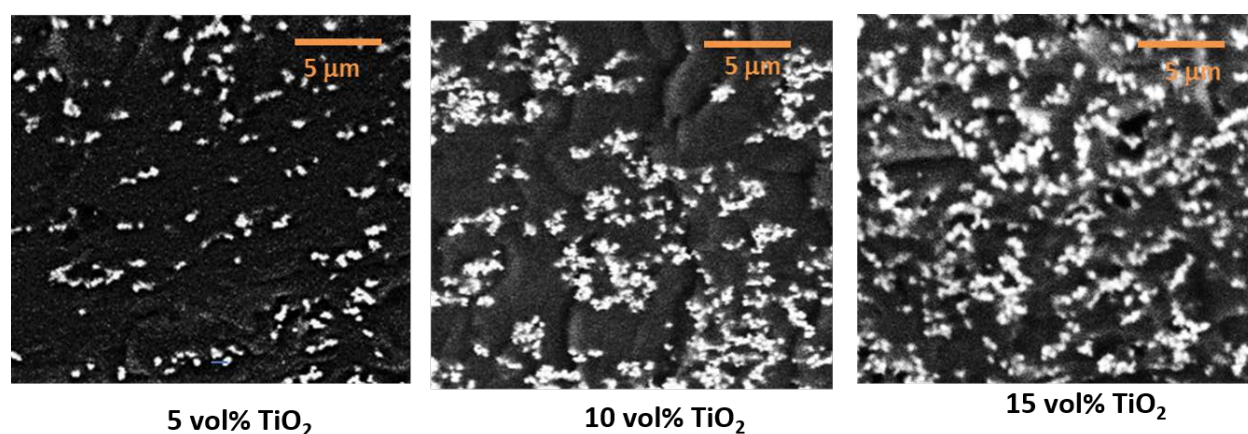


Figure 5. SEM micrographs for PU/TiO₂ nanocomposites for different composition, blow up on dispersed titania particles.

Dielectric Properties

Experience with the castor oil-based SECs led to believe that a decay in the materials' dielectric occurred over time, phenomenon never observed with SEBS-based SECs. We have studied the change in the relative permittivity over time by recording the value of ϵ_r over 3 weeks, by measuring the sensor's capacitance and back-calculating ϵ_r using equation (1). Figure 6 is a plot of the average value of relative permittivity for each set of specimens (no recording was taken for the 9th and 10th days). The decay of the dielectric value is evident, and stabilizes after approximately 16 days. Possible explanations include slow evaporation of the soluble

materials and reorganization of the filler. All tests discussed in this paper were performed on specimens older than 21 days to ensure a stable relative permittivity.

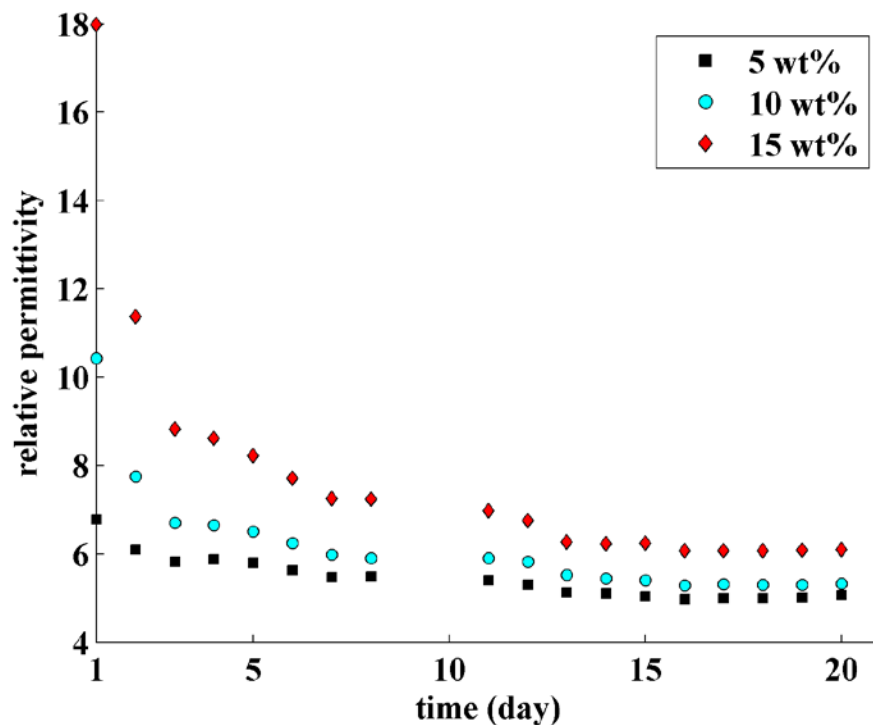


Figure 6. Average value of relative permittivity for each set over time

Thermogravimetric Analysis (TGA)

The thermal stability of PU/TiO₂ nanocomposites was investigated using thermogravimetric analysis (TGA, model Q50 from TA Instruments, New Castle, DE) over a temperature range of 30°C up to 700°C at 20°C/min under nitrogen atmosphere. Figure 8 shows a typical TGA measurement for PU/TiO₂ nanocomposites for different TiO₂ contents. Results show that the pure PU sample is thermally stable at a temperature range up to 250°C. Approximately 10 wt% of the sample is degraded at approximately 250–300°C. This process is related to the evaporation of soluble materials and unreacted oil fragments. With increasing the temperature up to 600 °C, two fast degradation processes were observed. The first one at the

temperature range of 300–380 °C, where approximately 60 wt% of the sample was lost due to the degradation of the polymer backbone. The second process at approximately 400–600 °C could be caused by further decomposition of the PU fragments. The multiple thermal degradation processes of bio-based polymers from vegetable oils are very common in literature. The thermal stability of these multiple degradation processes increased significantly (i.e., shifted to higher temperature ranges) by adding TiO₂ as seen in Figure 7. TiO₂ increases both the dielectric permittivity and the thermal stability of castor oil-based PU.

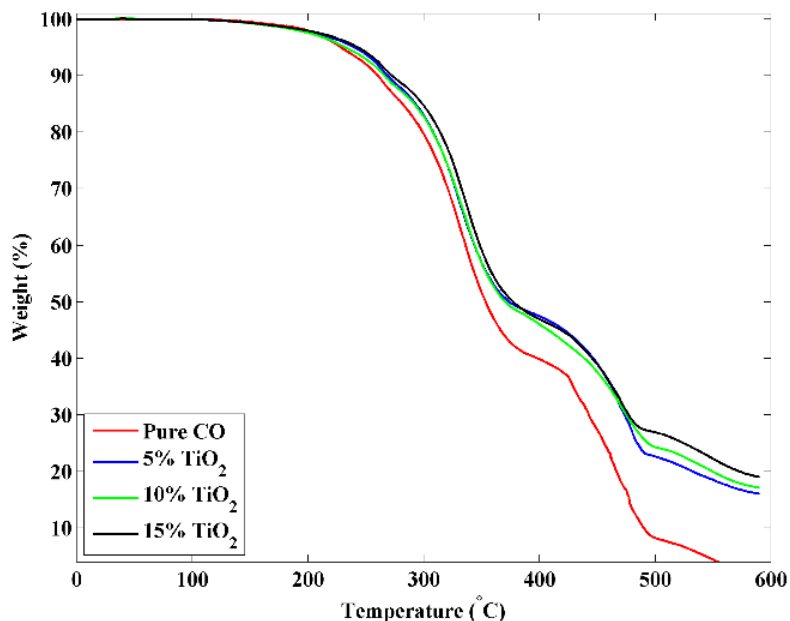


Figure 7. TGA measurements for PU/TiO₂ composites at 20°C/min heating rate under nitrogen atmosphere.

Laboratory Verifications

Experimental Setup

We conducted a free-standing sensor and a bending beam tests to validate the linearity of the proposed SEC over the range 0-6% strain, and verified the gauge factor (equation (7)) by deploying the sensor on a simply supported beam subjected to bending.

In the free-standing sensor test, three SEC with 5, 10, and 15 TiO₂ volume% were clamped separately into an Instron table-top mechanical testing machine (model 5569). Each of the sensor was subjected to six tensile strain cycles (from 1% to 6% strain with 1% strain increment), with each strain plateau attained at a loading rate of 5mm/min. This range of strain was governed by the allowable elongation of the testing equipment for the sample sizes, and is well beyond the failure point of typical structural materials. Data from the SECs were acquired using ACAM PCap01 sampled at 95.8 Hz . Figure 8 shows the laboratory setup for the free-standing sensor test. It is worth noting that equation (7) cannot be verified in a free-standing configuration because of the non-uniform distribution of strain within the dielectric.

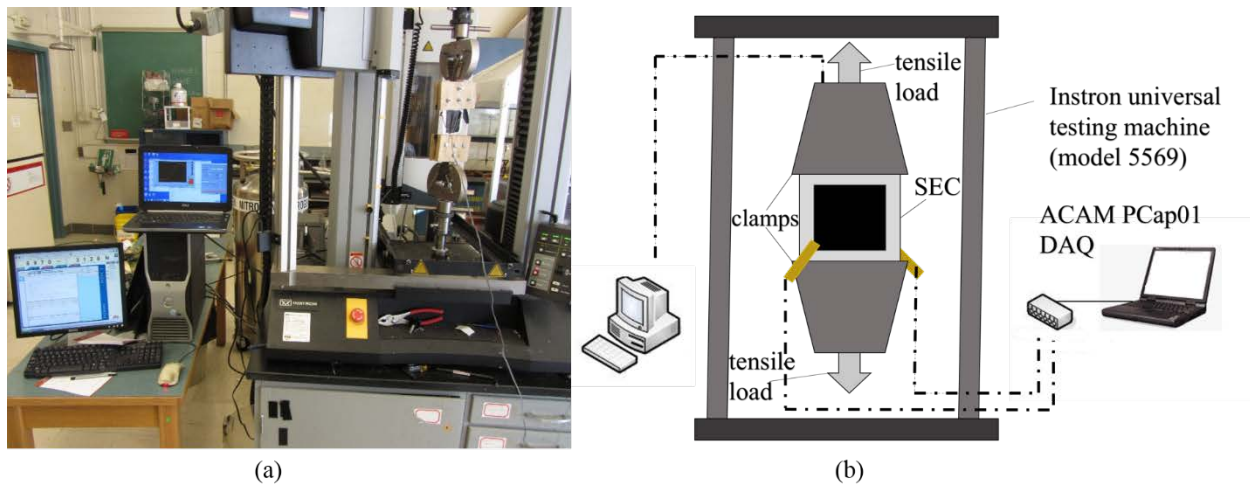


Figure 8. (a). Tensile test laboratory setup; (b) schematic of the clamped SEC on the Instron machine

In the bending beam test, the SEC specimens were installed onto the bottom surface of a simply supported aluminium plate of dimensions (36 x 8 x 0.25 in³) subjected to a four-point load setup as shown in figure 9. Each sensor was deployed within the uniform moment region using a thin layer of an off-the-shelf epoxy (JB Kwik) after sanding the plate surface and

applying a primer. Step loads (approximately 20 lb., 40 lb., 60 lb., and 80 lb.) were applied at 1/3 and 2/3 of the length of the plate using a hand operated hydraulic test system (Enerpac). Data from the SECs were acquired using an off-the-shelf DAQ (ACAM PCap01). Data from the RSGs were acquired using Hewlett-Packard 3852 DAQ.

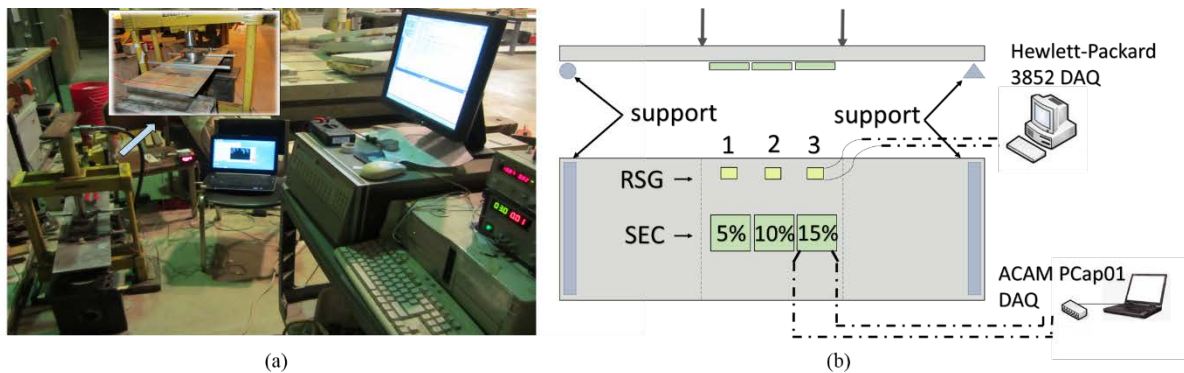


Figure 9. (a) Bending plate test laboratory setup; (b) schematic from side and under the plate (connection sensors-DAQ only shown for 2 sensors for clarity)

Results

Figures 10 and 11 show the results for the free-standing tests. Figure 10 compares time series of strain input and capacitance measurements. Time axes of strain and capacitance were manually aligned given the inaccurate synchronization of both DAQs. The comparison of time series measurements shows an agreement between the experimental values of strain and measured capacitance. There is an upwards slope in the capacitance measurements that becomes significant at high levels of strain. This slope is attributed to the viscoelastic behavior of the nanocomposite

Figure 11 is a plot of the normalized change in capacitance versus strain. Normalized measurements provide a better comparison given that equation (7) does not hold in a free-

standing configuration. Data are fitted linearly using a least square estimator. Results show that the sensor remains linear of the range 0-6% strain.

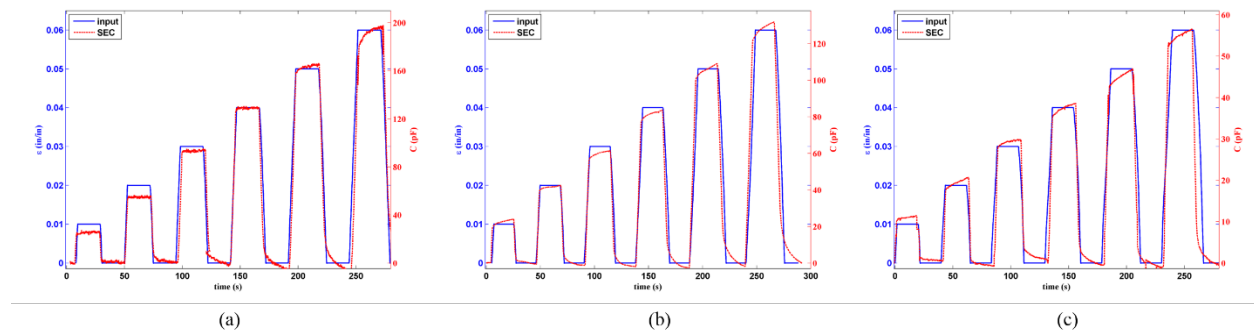


Figure 10. Strain history of SEC versus Instron RSG (free-standing test). (a) 5% TiO₂ content; (b) 10% TiO₂ content; (c) 15% TiO₂ content.

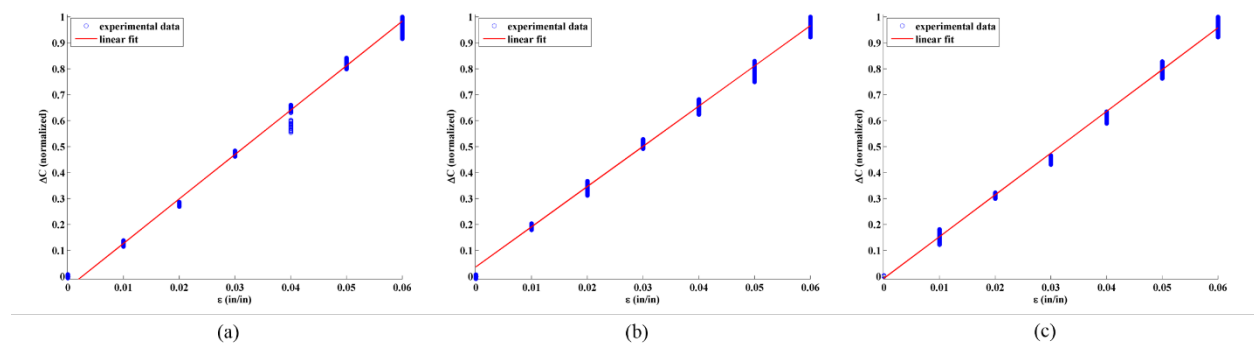


Figure 11. Verification of Linearity for free-standing bio-based SECs. (a) 5% TiO₂ content; (b) 10% TiO₂ content; (c) 15% TiO₂ content.

Figures 12 and 13 shows the results for the bending beam test. Comparison of time series data (Figure 12) also shows agreement between strain load and measured capacitance. A noticeable feature in the signals is a drift of the signal after each step load. We hypothesize that this drift is caused by the epoxy interface, which results in a slow relaxation process of the dielectric following a load step. The experimental gauge factor is obtained by plotting $\Delta C/C$ versus strain and taking the slope of the linear fit (Figure 13). Considering a value of $\nu_m = 0.33$ for aluminium and $\nu = 0.45-0.5$ for thermosets, the theoretical gauge factor of the castor oil-

based SEC is $1.34 < \lambda < 1.49$ (equation (7)). Table I summarizes the values obtained in Figure 13. The experimental gauge factors are all comprised within 1.34 and 1.49. Cross-specimens fluctuation can be explained by slight imperfections in the dispersion of the TiO₂, and changes in environmental conditions (temperature and humidity).

Table I. Strain gauge factors of SEC installed on an aluminium plate

	5%	10%	15%
Gauge factor λ	1.415	1.376	1.463

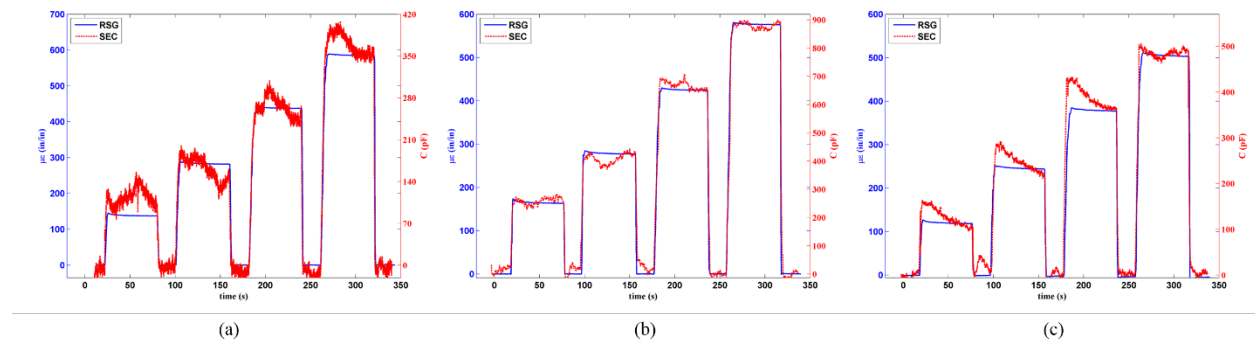


Figure 82. Strain history of SEC versus RSG (bending plate test). (a) 5% TiO₂ content; (b) 10% TiO₂ content; (c) 15% TiO₂ content.

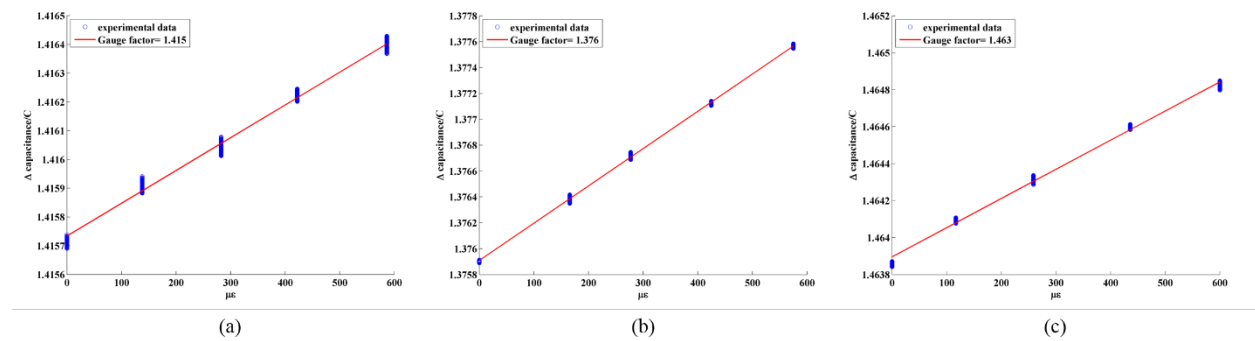


Figure 13. Verification of gauge factor for bio-based SEC (bending plate test). (a) 5% TiO₂ content; (b) 10% TiO₂ content; (c) 15% TiO₂ content.

Conclusion

In this paper, an inexpensive and bio-renewable material was presented to reduce the

environmental footprint of large area electronics. The proposed application is an SEC, constituted from a dielectric made of castor oil-based PU filled with titanium dioxide, and conductive plates made of SEBS filled with carbon black. Such sensor could be deployed in a large network configuration to cover large-scale surfaces, enabling monitoring of local strain over global areas.

The sensor showed to reach stability after approximately 16 days from fabrication. Scanning electron microscopy tests showed that all concentrations of TiO_2 (5%, 10%, and 15%) are dispersed well in the horizontal axis, but appear to have settled in the vertical axis. The thermogravimetric analysis showed good physical and chemical properties.

Static load tests were conducted on free-standing specimens and on specimens adhered onto an aluminium plate subjected to bending. Results from free-standing specimens showed that the sensor remained linear of the range 0-6% strain, and bending tests verified the theoretical gauge factor experimentally. These results confirmed the good dispersion of the particles within the castor oil PU and that the SEC can be used as a strain sensor.

The proposed castor oil-based SEC constitutes a promising sensor for monitoring of mesoscale surfaces. It demonstrates the utilization of bio-based polymers in the fabrication of sensors, which can result in important environmental benefits.

Acknowledgment

This work is supported by grant 13-02 from the Iowa Energy Center and grant 1001062565 from the Iowa Alliance for Wind Innovation; their support is gratefully acknowledged.

Reference

Blitz, Jack, and Geoff Simpson. *Ultrasonic methods of non-destructive testing*. Vol. 2. Springer, 1996.

Grosse, Christian U. *Acoustic emission testing*. Heidelberg: Springer, 2008.

Rens, Kevin L., Terry J. Wipf, and F. Wayne Klaiber. "Review of nondestructive evaluation techniques of civil infrastructure." *Journal of performance of constructed facilities* 11.4 (1997): 152-160.

Li, Hong-Nan, Dong-Sheng Li, and Gang-Bing Song. "Recent applications of fiber optic sensors to health monitoring in civil engineering." *Engineering structures* 26.11 (2004): 1647-1657.

López-Higuera, José Miguel, et al. "Fiber optic sensors in structural health monitoring." *Lightwave Technology, Journal of* 29.4 (2011): 587-608.

Glisic, Branko, and Yao Yao. "Fiber optic method for health assessment of pipelines subjected to earthquake-induced ground movement." *Structural Health Monitoring* 11.6 (2012): 696-711.

Laflamme, S., et al. "Soft capacitive sensor for structural health monitoring of large-scale systems." *Structural Control and Health Monitoring* 19.1 (2012): 70-81.

Hurlebaus, Stefan, and Lothar Gaul. "Smart layer for damage diagnostics." *Journal of intelligent material systems and structures* 15.9-10 (2004): 729-736.

Carlson, J. A., J. M. English, and D. J. Coe. "A flexible, self-healing sensor skin." *Smart materials and structures* 15.5 (2006): N129.

Tata, Uday, et al. "Bio-inspired sensor skins for structural health monitoring." *Smart Materials and Structures* 18.10 (2009): 104026.

Lipomi, Darren J., et al. "Skin-like pressure and strain sensors based on transparent elastic films of carbon nanotubes." *Nature nanotechnology* 6.12 (2011): 788-792.

Hu, Yingzhe, et al. "Large-Scale Sensing System Combining Large-Area Electronics and CMOS ICs for Structural-Health Monitoring." (2014): 1-12.

Zhou, Zhixiang, et al. "Smart film for crack monitoring of concrete bridges." *Structural Health Monitoring* 10.3 (2011): 275-289.

Gangopadhyay, Rupali, and Amitabha De. "Conducting polymer nanocomposites: a brief overview." *Chemistry of Materials* 12.3 (2000): 608-622.

Loh, Kenneth J., et al. "Carbon nanotube sensing skins for spatial strain and impact damage identification." *Journal of Nondestructive Evaluation* 28.1 (2009): 9-25.

Gao, Limin, et al. "Damage monitoring in fiber-reinforced composites under fatigue loading using carbon nanotube networks." *Philosophical Magazine* 90.31-32 (2010): 4085-4099.

Srivastava, Rajesh Kumar, et al. "The strain sensing and thermal–mechanical behavior of flexible multi-walled carbon nanotube/polystyrene composite films." *Carbon* 49.12 (2011): 3928-3936.

Kang, Inpil, et al. "A carbon nanotube strain sensor for structural health monitoring." *Smart materials and structures* 15.3 (2006): 737.

Arshak, K. I., D. McDonagh, and M. A. Durcan. "Development of new capacitive strain sensors based on thick film polymer and cermet technologies." *Sensors and Actuators A: Physical* 79.2 (2000): 102-114.

Suster, Michael, et al. "A high-performance MEMS capacitive strain sensing system." *Microelectromechanical Systems, Journal of* 15.5 (2006): 1069-1077.

Lipomi, Darren J., et al. "Skin-like pressure and strain sensors based on transparent elastic films of carbon nanotubes." *Nature nanotechnology* 6.12 (2011): 788-792.

Dobrzynska, Jagoda Anna, and M. A. M. Gijs. "Polymer-based flexible capacitive sensor for three-axial force measurements." *Journal of Micromechanics and Microengineering* 23.1 (2013): 015009.

Harrey, P. M., et al. "Capacitive-type humidity sensors fabricated using the offset lithographic printing process." *Sensors and Actuators B: Chemical* 87.2 (2002): 226-232.

Hong, Hyun Pyo, et al. "A highly fast capacitive-type humidity sensor using percolating carbon nanotube films as a porous electrode material." *Proc. IEEE Sensors*. 2012.

Madbouly, Samy A., Ying Xia, and Michael R. Kessler. "Rheological behavior of environmentally friendly castor oil-based waterborne polyurethane dispersions." *Macromolecules* 46.11 (2013): 4606-4616.

Xia, Ying, and Richard C. Larock. "Vegetable oil-based polymeric materials: synthesis, properties, and applications." *Green Chemistry* 12.11 (2010): 1893-1909.

Lu, Yongshang, and Richard C. Larock. "Soybean-oil-based waterborne polyurethane dispersions: effects of polyol functionality and hard segment content on properties." *Biomacromolecules* 9.11 (2008): 3332-3340.

Lu, Yongshang, et al. "Preparation and properties of starch thermoplastics modified with waterborne polyurethane from renewable resources." *Polymer* 46.23 (2005): 9863-9870.

Laflamme, Simon, et al. "Robust flexible capacitive surface sensor for structural health monitoring applications." *Journal of Engineering Mechanics* 139.7 (2012): 879-885.

Laflamme, Simon, et al. "Soft Elastomeric Capacitor Network for Strain Sensing Over Large Surfaces." (2013): 1-8.

Yang, Dan, et al. "A high-performance dielectric elastomer consisting of bio-based polyester elastomer and titanium dioxide powder." *Journal of Applied Physics* 114.15 (2013): 154104.

Saleem, H., et al. "Bio-inspired sensory membrane: Fabrication processes for full-scale implementation." *American Institute of Physics Conference Series*. Vol. 1511. 2013.

Kollosche, Matthias, et al. "Strongly enhanced sensitivity in elastic capacitive strain sensors." *Journal of Materials Chemistry* 21.23 (2011): 8292-8294.